Surface electron bands and Fermi surface of Be(0001)

I. Vobornik,[1] J. Fujii,[1] M. Mulazzi,[1,2] G. Panaccione,[1] M. Hochstrasser,[3] and G. Rossi[1,2]
[1]*TASC National Laboratory, CNR-INFM, S.S. 14, km 163.5, I-34012 Trieste, Italy*
[2]*Dipartimento di Fisica, Universita' di Modena e Reggio Emilia, Via Campi 213/A, I-41100 Modena, Italy*
[3]*Laboratorium für Festkörperphysik, Wolfgang-Pauli-Str. 16, ETH Hönggerberg, CH-8093 Zürich, Switzerland*
(Received 9 June 2005; published 25 October 2005)

The three surface electronic states of Be(0001) have different symmetry as probed by high-resolution angle resolved photoemission (ARPES) with variable polarization synchrotron radiation. We probed the two ($\bar{\Gamma}$-$\bar{M}$ and $\bar{\Gamma}$-K) high symmetry directions and measured the Fermi surface cuts. Electron states of even or odd symmetry with respect to the crystal (and/or surface) mirror planes contribute to the photoemission intensity as a function of the light polarization and experimental geometry. The effects of the large surface relaxation of Be(0001) are directly reflected in the Fermi surface.

DOI: 10.1103/PhysRevB.72.165424 PACS number(s): 73.20.At, 71.20.Gj, 71.18.+y, 79.60.Bm

I. INRODUCTION

The surface of Be(0001) is usually regarded as a characteristically different entity with respect to the bulk. It expands perpendicularly by $>4\%$,[1,2] which is the one of the largest surface expansions known. Beryllium has a closed shell $1s^2\,2s^2$ configuration. When the crystal is formed a significant fraction of the $2s$ electrons is promoted to $2p$ states. It was suggested that the p to s electron demotion at the surface accompanies this outward relaxation of the Be(0001) surface.[3]

The density of states (DOS) at the Fermi level is very low in bulk beryllium and there are large gaps in the electronic band structure. On the contrary the DOS is large at the surface due to the presence of surface states.[4] Three surface states have been identified in Be(0001). One lies in the Γ_3^+-Γ_4^- band gap, while there are both a surface state and a surface resonance in the M_2^--M_4^- band gap.

Furthermore large electron-phonon coupling is found at the Be(0001) surface.[5–8] This fact along with the high density of states at the Fermi level is predicted to be a candidate for showing surface superconductivity,[8] a phenomenon that up to now has not been confirmed by experiments.

Since the properties of Be are determined by the s to p electron transfer and its modification at the surface, it is important to understand the character of the states existing at the Be(0001) surface. Such a simple electron system, with only two electrons in the conduction band, can also serve as a model for understanding the origin of the valence band states.

We performed angle resolved photoemission with linearly polarized synchrotron radiation in the extreme ultraviolet range in order to measure the band structure along relevant symmetry directions, and, by reorienting the light polarization, to determine the symmetry of the electron states aiming to the recognition of their orbital character. Because of the extremely short mean free path ($\sim$2–3 Å) for the photoelectrons of 20–30 eV of kinetic energy in beryllium,[9,10] the surface to bulk ratio in the photoemission intensity is of the order of ten, and the information contained in the ARPES data as measured with $h\nu\sim30$ eV can be referred directly to the surface electronic structure.

We find that the surface state measured at the $\bar{\Gamma}$ point in the Brillouin zone (BZ) is mainly of s-p_z character, the surface states measured at $\bar{M}$ contain an important in-plane p component. The $\bar{\Gamma}$-$\bar{K}$ axes, that is not the crystal reflection axes, is the reflection axes for the surface and might introduce additional selection rules for the surface states. The measured Fermi surface cuts do show the main qualitative features of the three-dimensional (3D) bulk beryllium Fermi surface. The data indicate, however, that the Fermi surface topology is severely affected by the large surface relaxation.

II. EXPERIMENT

The ARPES experiments were performed at the low-energy (LE) branch of the APE-INFM beamline at the ELETTRA storage ring in Trieste. The APE-LE beamline delivers monochromatic synchrotron radiation in the energy range 10–100 eV from an Apple II-type quasiperiodic undulator with polarization control. In this experiment we used linearly polarized radiation oriented in the storage ring plane (also containing the surface normal and the symmetry axis of the analyzer) or perpendicular to it. We will call those cases linearly horizontal or linearly vertical polarized light. The ligh spot size on the sample is $\sim$150 μm and its size and position do not change when the polarization is changed. The angle of light incidence is 45°. Photoemission intensities and directions were measured by means of an electrostatic dispersive sector electron energy analyzer (Scienta SES2002) operated at an energy resolution of 20 meV (since our experiment was performed at room temperature the energy resolution did not need to be pushed further) and at an angular resolution of $\sim$0.2°.

We used the very same Be(0001) crystal on which the previous work was done by Hengsberger *et al.*[5,6] The atomically clean sample surface was obtained after several cycles of Ar^+ ion sputtering at 870 K and subsequent annealing at 700 K followed by slow cooling to room temperature. This procedure routinely leads to a sharp hexagonal low-energy electron diffraction pattern (LEED), while only minor carbon and oxygen contamination could be detected in the valence

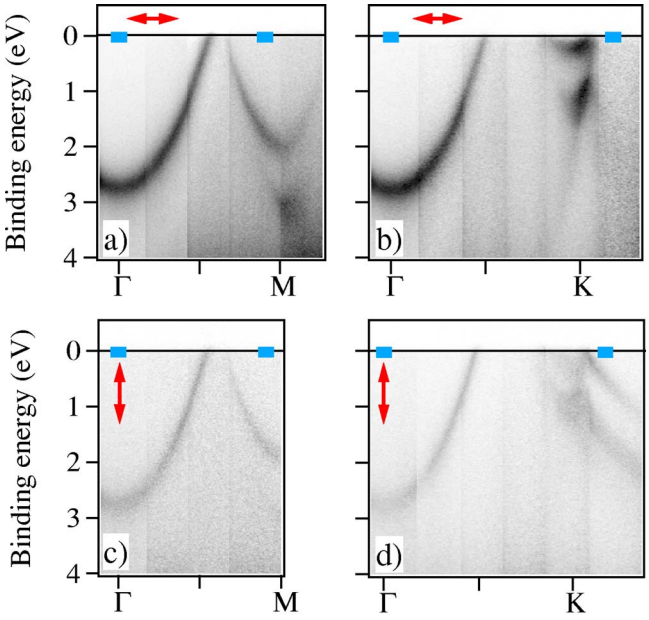

FIG. 1. (Color online) Energy dispersion curves for $h\nu$ =32.5 eV along $\bar{\Gamma}$-$\bar{M}$ and $\bar{\Gamma}$-$\bar{K}$ measured with horizontal (↔) (a), (b) and vertical (↕) (c), (d) polarization.

band spectra. The intensity of the $\bar{\Gamma}$ surface state photoemission was used as a criterion for the surface quality and of its ageing in the residual pressure of the sample environment $p<1\times10^{-10}$ mbar. The preparation procedure was repeated every three or four hours: during that time interval the surface state peak at normal emission ($\bar{\Gamma}$) is attenuated by 20%.

ARPES data were measured along the two ($\bar{\Gamma}$-$\bar{M}$ and $\bar{\Gamma}$-$\bar{K}$) high symmetry directions, as identified by LEED with an accuracy of ~2°. The two-dimensional electron detector at the exit plane of the SES2002 analyzer was set to display the photoelectron peak energy dispersion within an angular range of ~±7° about the nominal polar angle. By orienting the sample we could measure the dispersion over the whole high symmetry direction. We used the photon energies of 32.5 and 86 eV. The choice was made so as to be as close as possible to the two Γ points found experimentally by Jensen *et al.*[11,12] In addition, the Fermi surface cuts for the same photon energies were measured. In this case the angular resolution of ±1° was used and the data for every polar angle (changed in steps of 2°) are taken covering the whole (360°) azimuthal range.

III. RESULTS

Figure 1 shows the dispersion along the two ($\bar{\Gamma}$-$\bar{M}$,$\bar{\Gamma}$-$\bar{K}$) high symmetry directions measured with $h\nu$=32.5 eV and with horizontal and vertical polarizations. The main dispersive features visible along both directions are the surface states centered at $\bar{\Gamma}$ and at $\bar{M}$. The former disperses parabolically from ~2.75 eV below the Fermi energy and crosses the Fermi level at ~49% of the $\bar{\Gamma}$-$\bar{K}$ distance and ~58% of the $\bar{\Gamma}$-$\bar{M}$ distance. The later is parabolic about $\bar{M}$ where it

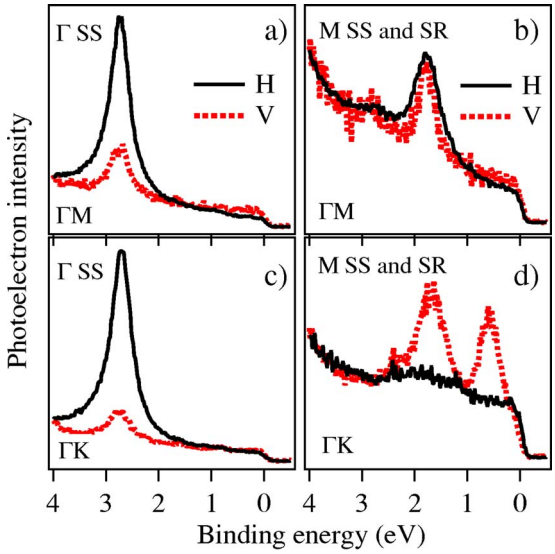

FIG. 2. (Color online) Comparison of the spectra measured with different polarizations and integrated over the regions marked with gray (blue) rectangles in Fig. 1 for the $\bar{\Gamma}$ surface state (SS) and $\bar{M}$ surface state and surface resonance (SS and SR) along $\bar{\Gamma}$-$\bar{M}$ (a), (b) and $\bar{\Gamma}$-$\bar{K}$ (c), (d); full black lines correspond to the horizontal (H) and dashed (red) lines to the vertical (V) polarization.

reaches ~1.95 eV binding energy. This state is visible in the dispersion along $\bar{\Gamma}$-$\bar{M}$, but also along $\bar{\Gamma}$-$\bar{K}$(-$\bar{M}$) in the case of vertical polarization. On the contrary, it is completely absent in the case of horizontal polarization. Besides the surface states, the remaining dispersive features close to $\bar{K}$ are the bulk bands [Figs. 1(b) and 1(d)]. The surface resonance at $\bar{M}$ is also visible for the vertical polarization along $\bar{\Gamma}$-$\bar{K}$-$\bar{M}$ as the second band dispersing below the $\bar{M}$ surface state [Fig. 1(d)].

When linearly polarized radiation is available, dipole selection rules can be exploited to determine the symmetry of states with respect to the mirror plane(s) of the crystal surface. In the case of emission in the crystal mirror plane, the final states are even with respect to the symmetry operations of that plane.[13] Then the nonvanishing matrix element for the dipole transition $\langle f|\mathbf{A}\cdot\mathbf{p}|i\rangle$ implies that the initial state must have the symmetry of the dipole operator $\mathbf{A}\cdot\mathbf{p}$. When measuring with horizontal (vertical) polarization, $\mathbf{A}\cdot\mathbf{p}$ is even (odd) and only the initial states of even (odd) reflection symmetry contribute to the emission.

The difference between the spectra taken with horizontal and vertical polarizations is seen in detail in Fig. 2, where the data integrated over the k-space areas marked by gray (blue online) rectangles in Fig. 1 are shown. It is visible in the spectra that $\bar{\Gamma}$ surface state peak measured with horizontal polarization is always more intense than the one measured with vertical polarization, implicating that this state is of even reflection symmetry. On the other hand the $\bar{M}$ surface state along $\bar{\Gamma}$-$\bar{M}$ results being of mixed even and odd symmetry, since the corresponding peaks are equally intense when measured with horizontal and vertical polarizations.

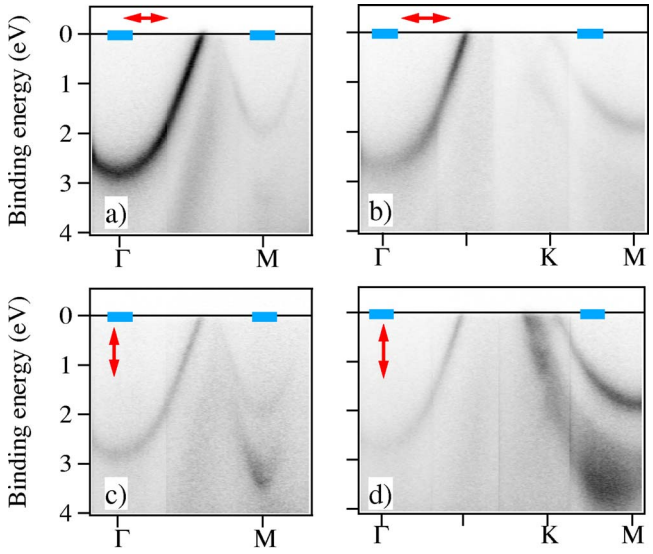

FIG. 3. (Color online) Energy dispersion curves for $h\nu$=86 eV along $\bar{\Gamma}$-$\bar{M}$ and $\bar{\Gamma}$-$\bar{K}$ measured with horizontal (↔) (a), (b) and vertical (↕) (c), (d) polarization.

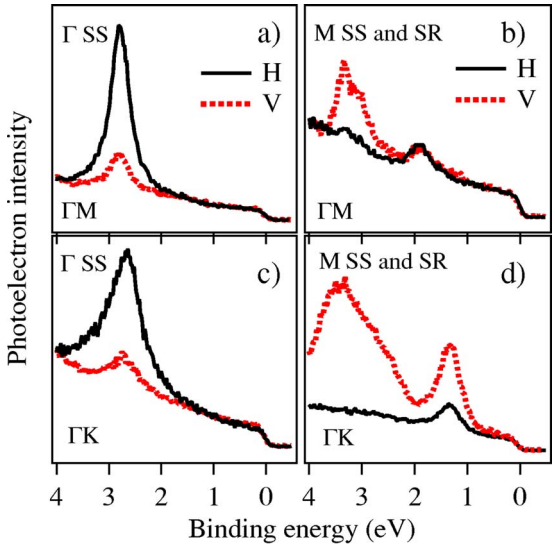

FIG. 4. (Color online) Comparison of the spectra measured with different polarizations and integrated over the regions marked with gray (blue) rectangles in Fig. 3 for the $\bar{\Gamma}$ surface state (SS) and $\bar{M}$ surface state and surface resonance (SS and SR) along $\bar{\Gamma}$-$\bar{M}$ (a), (b) and $\bar{\Gamma}$-$\bar{K}$ (c), (d); black full lines correspond to the horizontal (H) and dashed (red) lines to the vertical (V) polarization.

Along $\bar{\Gamma}$-$\bar{K}$ (as long as $\bar{\Gamma}$-$\bar{K}$ is treated as the surface reflection axes), only the states of odd reflection symmetry are present—in addition the background, there is practically no signal in the case of horizontal polarization.

Figure 3 illustrates the dispersion data along the two high symmetry directions taken with $h\nu$=86 eV. The main features observed in Fig. 1 are reproduced. However, the bulk bands close to $\bar{K}$ (in fact in this case they cross the Fermi level before reaching the $\bar{K}$ point) are not at all visible with the horizontal polarization, while they are strongly enhanced with the vertical polarization. For this photon energy the surface resonance at $\bar{M}$ is mixed with the bulk bands in the case of vertical polarization and is not visible in the case of horizontal polarization.

Similar to Fig. 2, Fig. 4 gives a collection of spectra integrated over the selected regions [gray (blue online) rectangles] of Fig. 3. The only qualitative difference with respect to the data in Fig. 2 is that now the $\bar{M}$ surface state along $\bar{\Gamma}$-$\bar{K}$ is visible as a weak peak also in the case of horizontal polarization, while the surface resonance is missing [Figs. 4(d) and Fig. 3(b)]. This may be a consequence of (i) different final states for the emission with 32.5 and 86 eV, of (ii) the uncertainty in the sample alignment (~2°), and of (iii) changed experimental geometry induced by the change in the Brillouin zone size when the photon energy is changed. In fact, in the case of 32.5 eV the angle between the (horizontal) polarization vector and the surface plane is 5° for the data relative to the $\bar{M}$ surface state; in the case of 86 eV this angle is 15° and consequently the out-of-surface-plane component of (horizontal) polarization is changed.

Figure 5 illustrates the Fermi surface cuts measured with $h\nu$=32.5 eV [Figs. 5(a) and 5(b)], $h\nu$=86 eV [Figs. 5(f) and 5(g)] and the two orthogonal polarizations. In order to visualize better the diversity between the data with different polarizations and photon energies, we plot also the corresponding sums [Fig. 5(c) for $h\nu$=32.5 eV and Fig. 5(h) for $h\nu$=86 eV] and differences [Fig. 5(d) for $h\nu$=32.5 eV and Fig. 5(i) for $h\nu$=86 eV]. In the case of a three-dimensional systems, the photoemission experiment with fixed photon energy measures a cut of the three-dimensional Fermi surface by the sphere defined by the Fermi energy (constant energy surface in the reciprocal space).

The data for $h\nu$=32.5 eV [Figs. 5(a)–5(d)] do reproduce the main features of the beryllium Fermi surface measured by de Haas–van Alphen effect.[14] The high intensity features close to $\bar{K}$ points are the cuts through the so-called cigars. The starlike features form the coronet, while the central circle is relative to the $\bar{\Gamma}$ surface state. In the case of vertical polarization the same features are reproduced, although the form and the relative intensities are not the same. The "cigars" are more extended away from $\bar{K}$. This additional intensity is due to the $\bar{M}$ surface state crossing close to $\bar{K}$. The coronet is almost completely missing and the circle corresponding to the $\bar{\Gamma}$ surface state has minima whenever $\bar{\Gamma}$-$\bar{M}$ line is approached. The intensity for the vertical polarization is, in this case, significantly lower than for the horizontal polarization, the sum and the difference of the data for the two polarizations do not differ significantly and are just slightly modified with respect to the data for horizontal polarization.

On contrary, the difference between the two polarizations is drastic for the case of $h\nu$=86 eV data, as can be seen in Figs. 5(f)–5(i). The horizontal polarization data are dominated by the surface state Fermi surface. For the vertical polarization the dominant feature is the one relative to the bulk cigar features, as seen also in the dispersion relation in Fig. 3. Only the sum of the data for the two polarizations

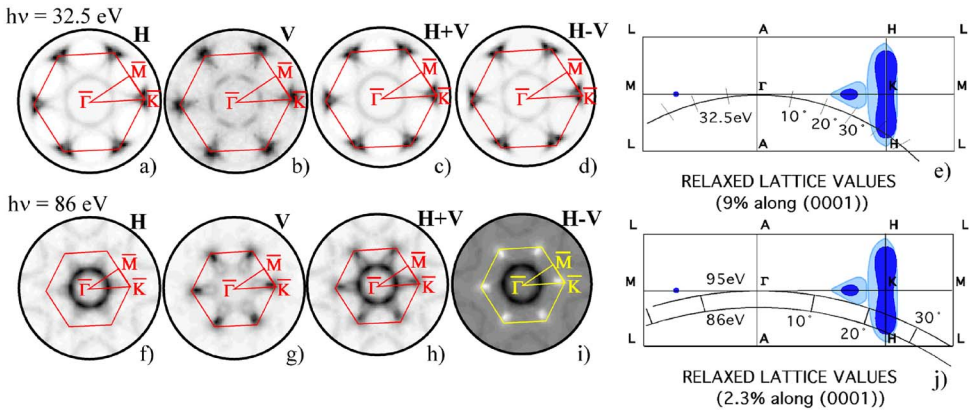

FIG. 5. (Color online) Fermi surface cuts measured with $h\nu$=32.5 eV and horizontal (H) (a) and vertical (V) (b) polarizations, their sum ($H+V$) (c) and difference ($H-V$) (d); Fermi surface cuts measured with $h\nu$=86 eV and horizontal (f) and vertical (g) polarizations, their sum ($H+V$) (h) and difference ($H-V$) (i); the hexagons in (a)–(d) and (f)–(i) delimit the first surface Brillouin zone; the arcs marked 32.5 eV in (e) and 86 eV in (j) denote the k-space area probed in our experiment; for more details see the text.

[Fig. 5(h)] contains all ingredients (coronet, cigars and the surface state Fermi surface) of the beryllium Fermi surface. Since the intensity of the surface state with horizontal polarization and the intensity of the cigar features with vertical polarization is comparable, the difference plot [Fig. 5(i)] contains both negative (white) and positive features (black), corresponding to the cigars and surface state, respectively.

In order to get more information about the Fermi surface topology, one needs to understand where exactly the three-dimensional Fermi surface is cut in our experiment. This is illustrated in Figs. 5(e) and 5(j), in the Γ-K-H-A reciprocal-space plane. The light gray (light blue online) features correspond to the Fermi surface measured by de Haas–van Alphen oscillations,[14] while the dark gray (dark blue online) features are the calculated Fermi surface using the Slater-Koster scheme.[15] We used an inner potential of 11.1 eV, a work function of 5.1 eV, and assuming the free electron final state we determined the constant energy surfaces corresponding to 32.5, 86, and 95 eV excitation energies [arcs in Figs. 5(e) and 5(j)].

Experimentally, measuring the dispersion along the Δ line, Jensen *et al.*[11] found the two nearest Γ points at 32.5 and 95 eV. Using the bulk lattice constants with the above-mentioned assumptions, the curves corresponding to 32.5 and 95 eV are far from the Brillouin zone centers. The only way to reach the two Γ points with 32.5 and 95 eV is to assume $9\pm2\%$ relaxation for 32.5 eV and $2.3\pm2\%$ relaxation for 95 eV.[16]

Taking into account the very short mean free path for electrons with ~30 eV kinetic energy[9,10] and that the total surface expansion may range from 2.6–9 % (the error bar limits of Ref. 2) the result of the surface expansion probing with 32.5 eV light energy is within range of previous experimental and theoretical work.[1–3] The available data for the electron mean free path are limited to about 55 eV of maximum kinetic energy: in these conditions the surface to bulk intensity ratio is reduced to below 2. By extrapolating this trend to ~82 eV of kinetic energy we can understand the bulk electron states to contribute significantly in the valence band spectra and Fermi surfaces of Be(0001).

From these plots the curves corresponding to both 32.5 and 86 eV cut the "cigar" (elongated) Fermi surface features only. The data of Fig. 5, nevertheless, show clear coronet features, in particular for the case of 32.5 eV. If further the band dispersion of Fig. 4 is looked more in detail, one sees that the bulk bands crossing occurs before the $\bar{K}$ point is reached. This is possible only if the 86 eV cut were tangential to the lowest extreme of the cigar feature and that would imply the cigar feature to be shorter by ~20%. On the other hand the coronets should be at least 50% larger to be seen with both 32.5 and 86 eV. This indicates that the bulk Fermi surface of beryllium is quite different at the surface, due to the surface relaxation, and that the rigid shift model of de Haas–van Alphen bulk structures provides only a rough guideline for understanding the surface electronic structure of Be(0001).

We note that in Figs. 5(e) and 5(j), the Fermi surfaces are shrunk in the ΓA direction by the same amount as the inverse lattice. This is obviously a very crude first approximation since the effects of lattice-dimension changes combined with changes in the electron density can have strong effects on the Fermi surface.[14] In the calculations by Feibelman,[3] it is pointed out, that there is in fact a significant electron density change in relaxed Be crystal. In addition, there is quite a difference between the measured Fermi surface by the de Haas–van Alphen effect and the calculated one. To fully understand the Fermi surfaces modification, more advanced Fermi surface calculations are necessary accompanied by the Fermi surface cuts measured at more excitation energies.

IV. DISCUSSION

The electronic band structure of Be(0001) was measured by photoemission in the past and compared to band structure calculations.[11,17–19] In particular the surface state bands were studied in detail when the issue of possible surface superconductivity attracted a lot of attention.[5–8] However, in addition to the work of Karlsson *et al.*,[19] where the symmetry of the $\bar{\Gamma}$ surface state was examined, none of the previous studies

concentrated on the symmetry of the initial states.

With the symmetry argument in mind, the data of Figs. 1–4 imply that the $\bar{\Gamma}$ surface state band is of even reflection symmetry and consequently mixed s and p_z character, with a minor (if any) contribution of the in-plane p states, relative to the intensity measured with vertical polarization. In fact it is likely that the $\bar{\Gamma}$ surface state intensity measured with the vertical polarization in the crystal reflection plane (along $\bar{\Gamma}$-$\bar{M}$ is even more suppressed than what is seen in Figs. 2 and 4. This can be deduced from the Fermi surface measured with $h\nu$=32.5 eV with vertical polarization [Fig. 5(b)] that shows marked minima in the surface state Fermi surface whenever $\bar{\Gamma}$-$\bar{M}$ is crossed. This discrepancy between the $\bar{\Gamma}$ surface state data of Figs. 1 and 2 and Fig. 5(b) is due to the uncertainty in the sample azimuthal alignment. We remind the reader, however, that the misalignment is small ($\sim 2°$), as seen from the measured band minima for the $\bar{M}$ surface state and surface resonance (Figs. 1 and 2), which are consistent with the photoemission data from other groups[18] and the band structure calculations.[3,4] The minima in the Fermi surface of Fig. 5(b) identify in fact the $\bar{\Gamma}$-$\bar{M}$ high symmetry direction as the one in the crystal reflection plane.

On the other hand, the $\bar{M}$ surface state along $\bar{\Gamma}$-$\bar{M}$ is of mixed even and odd reflection symmetry [the intensities for the two polarizations are the same; Figs. 2(b) and 4(b)]. The electrons in the vicinity of the Fermi level are either of 2s or 2p origin, but the only states that can have odd reflection symmetry are the in-plane p states and this implies an important contribution of the in-plane p states to the $\bar{M}$ surface state.

This surface state is almost completely absent along $\bar{\Gamma}$-$\bar{K}$ with the horizontal polarization and clearly visible with vertical polarization. One could argue that the $\bar{\Gamma}$-$\bar{K}$ axes is not in the crystal reflection plane and therefore the symmetry selection rules (that are valid for the emission in the reflection plane) do not apply. We nevertheless remind that also the $\bar{\Gamma}$ surface state along $\bar{\Gamma}$-$\bar{K}$ is subject to the important intensity suppression when the polarization is changed to vertical although $\bar{\Gamma}$-$\bar{K}$ is not the crystal reflection axes. The fact that $\bar{\Gamma}$-$\bar{K}$ is placed in the surface reflection plane might introduce extra selection rules for the surface states [in particular for the ones strongly localized at the surface as the $\bar{\Gamma}$ surface state of Be(0001) (Ref. 4)]. We in fact see similar intensity suppression in the Cu(111) surface state both along $\bar{\Gamma}$-$\bar{M}$ in the crystal reflection plane) and $\bar{\Gamma}$-$\bar{K}$ (not in the crystal reflection plane).[20] Concerning Be(0001), if the emission along $\bar{\Gamma}$-$\bar{K}$ could be treated as the emission in the reflection plane, this would still imply a significant contribution of the in-plane p states for the $\bar{M}$ surface state, as concluded from the data along $\bar{\Gamma}$-$\bar{M}$.

Independent of symmetries, the intensity variation as a function of polarization is strictly related to the photoemission matrix element and requires more rigorous theoretical treatment. Consequently more attention should be dedicated to the photoemission final states. This is seen also in the measured Fermi surface cuts, in particular in the case of $h\nu$=86 eV, where the cigar related features, that are dominant with vertical polarization, disappear completely with horizontal polarization.

Different band structure calculations fit well to the measured ARPES data. The linearized-augmented-plane-wave calculation by Feibelman,[3] concentrated mainly at understanding of the geometric and electronic structure of Be(0001) and of the large surface expansion, deals also with the symmetry of surface states. The $\bar{\Gamma}$ surface state is considered to be of sp_z character while the $\bar{M}$ surface states are mainly of the $sp_{x,y}$ origin, which is consistent with our polarization-dependent data.

V. CONCLUSIONS

In summary, the direct sensitivity to symmetry of the initial electron states obtained by polarization dependent photoemission, allowed us to find that the $\bar{\Gamma}$ surface state is mainly of s-p_z character, while the $\bar{M}$ surface state has an important mixture of the in-plane p states. These results confirm theoretical predictions. Drastic changes were measured in the Fermi surface as a function of photon polarization calling for a detailed theoretical evaluation of the photoemission matrix elements in the relevant experimental geometries. The measured Fermi surface cuts demonstrate how the Fermi surface mapping by ARPES with polarized light is directly related to the surface electronic structure in a system such as Be(0001).

ACKNOWLEDGMENTS

We are pleased to acknowledge P. Aebi for kindly letting us use the Be(0001) crystal from his Laboratory. We thank D. Krizmancic for the acquisition and beamline control software support.

[1] H. L. Davis, J. B. Hannon, K. B. Ray, and E. W. Plummer, Phys. Rev. Lett. **68**, 2632 (1992).

[2] K. Pohl, J.-H. Cho, K. Terakura, M. Scheffler, and E. W. Plummer, Phys. Rev. Lett. **80**, 2853 (1998).

[3] P. J. Feibelman, Phys. Rev. B **46**, 2532 (1992).

[4] E. V. Chulkov, V. M. Silkin, and E. N. Shirykalov, Surf. Sci. **188**, 287 (1987).

[5] M. Hengsberger, D. Purdie, P. Segovia, M. Garnier, and Y. Baer, Phys. Rev. Lett. **83**, 592 (1999).

[6] M. Hengsberger, R. Fresard, D. Purdie, P. Segovia, and Y. Baer, Phys. Rev. B **60**, 10 796 (1999).

[7] S. LaShell, E. Jensen, T. Balasubramanian, Phys. Rev. B **61**, 2371

(2000).
[8] T. Balasubramanian, E. Jensen, X. L. Wu, and S. L. Hulbert, Phys. Rev. B **57**, R6866 (1998).
[9] L. I. Johansson and B. E. Sernelius, Phys. Rev. B **50**, 16 817 (1994).
[10] L. I. Johansson, H. I. P. Johansson, J. N. Andersen, E. Lundgren, and R. Nyholm, Phys. Rev. Lett. **71**, 2453 (1993).
[11] E. Jensen, R. A. Bartynski, T. Gustafsson, E. W. Plummer, M. Y. Chou, Marvin L. Cohen, and G. B. Hoflund, Phys. Rev. B **30**, 5500 (1984).
[12] Note that 86 eV is the last photon energy that allows for controllable change of photon polarization. That is the reason we did not use 95 eV, as determined by Jensen *et al.*, but 86 eV.
[13] Stefan Hüfner, *Photoelectron Spectroscopy* (Springer, Berlin, 1996).
[14] J. H. Tripp, P. M. Everett, W. L. Gordon, and R. W. Stark, Phys. Rev. **180**, 669 (1969), and references therein.
[15] T.-S. Choy, J. Naset, J. Chen, S. Hershfield, and C. Stanton, Bull. Am. Phys. Soc. **45** (1), L36 42 (2000).
[16] Note that the error in the relaxation is associated with the choice of the inner potential, the work function and the assumption of a free electron final state.
[17] E. Jensen, R. A. Bartynski, T. Gustafsson, and E. W. Plummer, Phys. Rev. Lett. **52**, 2172 (1984).
[18] R. A. Bartynski, E. Jensen, T. Gustafsson, and E. W. Plummer, Phys. Rev. B **32**, 1921 (1985).
[19] U. O. Karlsson, S. A. Flodström, R. Engelhardt, W. Gädeke, and E. E. Koch, Solid State Commun. **49**, 711 (1984).
[20] M. Mulazzi, J. Fujii, I. Vobornik, G. Panaccione, and G. Rossi (unpublished).